Journal of Sound and Vibration (1980) **71**(3), 399–419

A REVIEW OF PROPELLER DISCRETE FREQUENCY NOISE PREDICTION TECHNOLOGY WITH EMPHASIS ON TWO CURRENT METHODS FOR TIME DOMAIN CALCULATIONS

F. FARASSAT†

Joint Institute for Advancement of Flight Sciences, The George Washington University, Hampton, Virginia 23665, *U.S.A.*

AND

G. P. SUCCI‡

Department of Aeronautics and Astronautics, Massachusetts Institute of Technology, Cambridge, Massachusetts 02139, *U.S.A.*

(*Received* 3 *October* 1979, *and in revised form* 16 *February* 1980)

A review of propeller noise prediction technology is presented which highlights the developments in the field from the successful attempt of Gutin to the current sophisticated techniques. Two methods for the prediction of the discrete frequency noise from conventional and advanced propellers in forward flight are described. These methods developed at MIT and NASA Langley Research Center are based on different time domain formulations. Brief description of the computer algorithms based on these formulations are given. The output of these two programs, which is the acoustic pressure signature, is Fourier analyzed to get the acoustic pressure spectrum. The main difference between the programs as they are coded now is that the Langley program can handle propellers with supersonic tip speed while the MIT program is for subsonic tip speed propellers. Comparisons of the calculated and measured acoustic data for a conventional and an advanced propeller show good agreement in general.

1. INTRODUCTION

The technology for propeller noise prediction has been under development for many years. There is a new interest in accurate prediction methods for propeller noise because of the public pressure to reduce noise pollution and to meet government noise regulations. This paper presents two basically equivalent methods which were developed at Langley and at MIT respectively, and which have been used very successfully in predicting the noise of propellers. The success of these methods depends on the selection of appropriate acoustic formulations and the computer algorithms to implement these formulations. Before these methods are discussed in detail a short review of previous attempts to predict propeller noise will be presented.

2. REVIEW OF PREDICTION TECHNOLOGY DEVELOPMENT

A good review of aerodynamic sound of rotating blades was published by Morfey [1]. In the following, the emphasis will be on prediction techniques only. Propeller noise

† Currently with the Acoustics and Noise Reduction Division, NASA-Langley Research Center, Mail Stop 461, Hampton, Virginia 23665, U.S.A.

‡ This work was partially completed when the author was Visiting Research Scientist at the Joint Institute for Advancement of Flight Sciences.

0022–460X/80/150399+21 $02.00/0

generation has a great deal of similarity to those of other members of rotating blade machinery such as fans and helicopter rotors. Often research findings on fans and rotors have resulted in a better understanding of propeller noise generation and thus improving its prediction.

The first successful prediction theory was by Gutin [2]. Gutin replaced the effect of blade forces on the fluid by a distribution of oscillating forces in the propeller disk. He then used a result of Lamb for the acoustic field of a stationary oscillating point force, and the superposition principle, to calculate the level of the harmonics of the acoustic pressure. The success of this theory to calculate the first few harmonics of propellers with low tip speed is well known. Only loading noise, that is the noise due to the forces on the fluid, was considered by Gutin.

Ernsthausen in Germany [3] and Deming in the U.S. [4] were among the first researchers to recognize the importance of noise generated by virtue of the finite blade thickness. Ernsthausen qualitatively explained the origin and characteristics of this noise. However, it was Deming who correctly formulated this problem theoretically. Each blade segment is assumed to generate a periodic disturbance in the propeller disk which can be Fourier analyzed into stationary but pulsating distributed sources along the path of the blade segment. Deming converted the problem of the determination of the sound generated by a non-lifting blade into the equivalent problem of the sound from a continuous distribution of piston sources radiating into a half-space. Using the superposition principle he obtained an expression for the far-field thickness noise. Because of the limited computing capability of the 1930's, Deming had to make some simplifying assumptions in his acoustic calculations. He obtained generally good agreement with experimental data up to the highest test tip Mach number of about 0·7.

Another significant step in the prediction of the noise of propellers was taken by Garrick and Watkins [5]. They extended the work of Gutin to propellers in forward flight. The acoustic sources were again distributed on the entire propeller disk. Each source on the disk travels rectilinearly. A simple geometrical construction was used to obtain the source position at the emission time and the relative position of the source and the observer used in acoustic calculations. This geometrical construction is sometimes called the Garrick triangle. Garrick and Watkins considered loading noise in their analysis although their method could be used to extend Deming's thickness noise analysis to propellers in forward flight.

In the mid-fifties, Arnoldi obtained an expression for thickness noise in the frequency domain [6]. His result was developed for compact blade sources in contrast to Deming's analysis which was for non-compact sources. Arnoldi's expression is relatively simple and is comparable to Gutin's result for the loading noise.

In the early sixties, Van de Vooren and Zandbergen obtained a solution for the acoustic field of a singularity in helical motion [7]. They applied this solution to calculate the thickness and loading noise of propellers in forward flight. Although their numerical results are for a single singularity, in principle their method can be used for a surface distribution of sources by dividing the blades into panels and using the superposition principle. Unfortunately the above method, which requires a computer for acoustic calculations, did not receive proper attention.

Since the early sixties, considerable research has been done on the understanding of the noise mechanisms and the prediction of the noise of rotating blades. The development of high speed digital computers helped the researchers to use more realistic models in their study. Some of the more recent developments in mathematics, such as generalized function theory, simplified the process of finding the solution of the wave equation of acoustics with moving volume and surface sources. One successful attempt was the

solution obtained by Lowson for a moving point source [8]. His simple, but powerful, result for a point force in motion, incorporates much of the earlier results which were obtained by classical mathematics. Using more sophisticated mathematics Ffowcs Williams and Hawkings published a paper in which they derived the now famous Ffowcs Williams–Hawkings (FW–H) equation [9]. The acoustic analogy was applied to obtain a wave equation for the fluid density in the medium around a body in arbitrary motion. Although reference to turbulence is made in the title of this paper, the current applications of the theory of these authors are limited to surface sources. One significant contribution of Ffowcs Williams and Hawkings was to write their solution of the acoustic wave equation (FW–H equation) in various forms. In a particular problem, some of these forms are more appropriate than others. It is less known that a paper published by Möhring, Müller and Obermeier at about the same time that the paper by Ffowcs Williams and Hawkings appeared, is closely related to the latter authors' work [10].

When acoustic sources are in motion, the spatial extent of the source to an observer who receives the sound can change considerably. If the source motion, its frequency of fluctuations and the observer position are such that the source can be treated as a moving point source, it is said to be compact. Otherwise it is non-compact. Ffowcs Williams and Hawkings formalized the treatment of the acoustics of non-compact sources. The two prediction methods discussed here are for non-compact sources.

Up to the late sixties, it was believed that the thickness noise of rotating blades was not significant enough to be included in acoustic calculations. This belief, based partly on qualitative reasoning, could not be justified because of the evidence to the contrary in the published literature. The works of Arnoldi [6] and Van de Vooren and Zandbergen [7] indicated that thickness and loading noise components can be of comparable magnitude for typical operating conditions of a propeller. More recently, Lyon found by a numerical method that the thickness noise can be the dominant noise component in the plane of a helicopter rotor at high blade tip speeds [11]. This conclusion, of course, applies directly to the propeller noise problem. Since the publication of that paper, many other workers in this field have derived various equivalent formulations of thickness noise [12–19]. These formulations, together with those for non-compact loading noise, can all be related to the various forms of the solution of the FW–H equation. There are some approximations involved in most of the current numerical methods. These approximations concern the blade surface representation and retarded time calculation for sources on the blade. They can account for small variations in the results of various techniques. It is interesting to note that Hanson has successfully adapted his frequency domain method for aeroacoustic design of high speed propellers [18]. Jou has extended the work of Hawkings and Lowson [12] to propellers in forward flight [19]. Some interesting qualitative results were obtained by Jou which give insight into noise generation aspect of high speed propellers. No extensive numerical computations or comparison with experimental results have been published in which Jou's formulation has been used.

One discovery that has important bearing on the work presented here was that static propellers generated more noise than propellers in forward flight. Similar behavior has also been observed for the fan of turbofan engines. It was Hanson's idea that the discrepancy, which was observed at high harmonics of the measured sound, was due to differences in fluctuating load levels in the cases of static fans and those in forward flight [20]. In the case of static fans, the turbulent eddies are stretched to considerable length while being sucked into the fan, and thus cause fluctuating forces on the blades. Fans in flight fly into the turbulent eddies thus giving them much less time to stretch out and to cause fluctuating blade loading. This idea of Hanson has been verified by experiments with instrumented blades. A similar study on propellers by Hamilton Standard for NASA

established that the same phenomenon is also at work in propellers [21, 22]. The importance of fluctuating blade loading on noise generated by helicopter rotors has also been known for many years. In the case of propellers, noise measured in the regions where the surface sources appear compact is influenced greatly by fluctuating blade loading. For conventional static propellers, high harmonics of measured sound are primarily due to fluctuations in blade loading even where steady blade loading and thickness sources are non-compact. A compact source calculation for fluctuating blade loading together with a non-compact source calculation for thickness and steady loading noise appears to be the best approach for predicting the noise of static propellers [22].

The latest development in this field has been the realization of the importance of non-linearities in the flow field around the blades [23, 24]. Some non-linear effects can be inferred when linear acoustic calculations are compared with measured propeller noise data. For instance, the calculated width of the acoustic pressure signature is narrower than the measured width. For conventional propellers this difference does not appear to be significant. However, one phenomenon, when not taken into consideration in linear acoustic calculations, can lead one to suspect erroneously the importance of non-linear effects. This phenomenon is the interaction of propeller blades with the flow field established around the aircraft nacelles, wings and fuselage. The blades sense a periodic load, once per revolution, due to asymmetry in the airflow into the propeller. This blade load variation increases the levels of most harmonics of the acoustic pressure spectrum. In the examples presented in this paper for a general aviation propeller, these blade load variations are included in calculations and they have noticeable effect on the results.

As discussed above, there have been considerable gains in knowledge and experience on propeller noise. It is now possible to calculate propeller noise with good accuracy. In this paper two related methods with different capabilities are presented. In studying the acoustics of rotating blades it becomes obvious that a closed form analytic solution always requires some unwanted restrictions such as far field positioning of the observer. The frequency domain approach restricts the observer to move with the propeller [5, 18]. To have the least restrictive prediction method, a time domain numerical approach seems the best choice and those reported here are time domain methods.

In the next section, the analytic formulations are derived. Brief descriptions of algorithms used in the computer codes are then presented. The inputs to these programs are blade geometry, loading and the propeller motion. The acoustic pressure signature and spectrum are the outputs. These programs are identified as the MIT and the Langley programs.

To demonstrate the applications of these programs, several examples related to a series of flight tests on a three bladed propeller will be presented. One of the blades was instrumented with pressure gauges which responded to the fluctuations in surface pressure. It was found that each blade experiences a large fluctuating load with fundamental frequency equal to the shaft frequency. This fluctuation was caused by non-uniform flow into the propeller due to the presence of the wing and engine intake blockage. Both steady and fluctuating loads were included in the calculations. The agreement of theoretical and measured data is generally good. The MIT program was used for these calculations.

Some calculated acoustic pressure signatures and spectra of a propeller with advanced blade geometry (prop-fan) operating at supersonic tip speed are presented. These were computed by means of the Langley program. In general the agreement with the experimental data is good. Some non-linear effects are observed which are discussed in the paper.

3. THEORETICAL FORMULATIONS

In this section the formulations used in the noise prediction programs will be presented. The starting point of the analysis is the FW–H equation without the quadrupole term [9],

$$\frac{1}{c^2}\frac{\partial^2 p'}{\partial t^2}-\nabla^2 p'=\frac{\partial}{\partial t}[\rho_0 v_n|\nabla f|\delta(f)]-\frac{\partial}{\partial x_i}[l_i|\nabla f|\delta(f)], \tag{1}$$

where p' is the acoustic pressure, ρ_0 and c are the density and speed of sound in the undisturbed medium respectively, v_n is the local normal velocity on the surface of a given body $f(\mathbf{x}, t)=0$ in motion. The local force on the fluid (per unit area) at the surface of the body is denoted by l_i and $\delta(f)$ stands for the Dirac delta function.

The solution of equation (1) of interest here has been published elsewhere [13, 25]. The derivation will not be repeated here. The solution can be written in terms of two integrals over the surface Σ, which is defined by $F(\mathbf{y}; \mathbf{x}, t)=f(\mathbf{y}, t-r/c)=[f(\mathbf{y}, \tau)]_{\text{ret}}=0$, where $r=|\mathbf{x}-\mathbf{y}|$. It is

$$4\pi p'(\mathbf{x}, t)=\frac{1}{c}\frac{\partial}{\partial t}\int_{F=0}\frac{1}{r}\left[\frac{\rho_0 c v_n+1_r}{\Lambda}\right]_{\text{ret}}\mathrm{d}\Sigma+\int_{F=0}\frac{1}{r^2}\left[\frac{1_r}{\Lambda}\right]_{\text{ret}}\mathrm{d}\Sigma, \tag{2}$$

where $l_r=l_i\hat{r}_i$ and $\hat{r}_i=(x_i-y_i)/r$ is the unit vector in the radiation direction. Here $\Lambda^2=1+M_n^2-2M_n\cos\theta$ where $M_n=v_n/c$ and θ is defined below. If $\mathrm{d}S$ is the element of the surface area of the body $f=0$ and $\mathrm{d}\Gamma$ is an element of the length of the curve of intersection of this body and the sphere $g=\tau-t+r/c=0$, then it can be shown that

$$\mathrm{d}\Sigma/\Lambda=\mathrm{d}S/|1-M_r|=c\,\mathrm{d}\Gamma\,\mathrm{d}\tau/\sin\theta, \tag{3a, b}$$

where $M_r=v_i\hat{r}_i/c$, v_i is the local velocity of the body surface and θ is the angle between the outward normal to the body surface and r_i. The source time is denoted by τ. By using equation (3) in equation (2), the following two equations are obtained:

$$4\pi p'(\mathbf{x}, t)=\frac{1}{c}\frac{\partial}{\partial t}\int_{f=0}\left[\frac{\rho_0 c v_n+1_r}{r|1-M_r|}\right]_{\text{ret}}\mathrm{d}S+\int_{f=0}\left[\frac{1_r}{r^2|1-M_r|}\right]_{\text{ret}}\mathrm{d}S, \tag{4a}$$

$$=\frac{\partial}{\partial t}\int_{\substack{f=0\\g=0}}\frac{\rho_0 c v_n+1_r}{r\sin\theta}\mathrm{d}\Gamma\,\mathrm{d}\tau+\int_{\substack{f=0\\g=0}}\frac{c\,1_r}{r^2\sin\theta}\mathrm{d}\Gamma\,\mathrm{d}\tau. \tag{4b}$$

Depending on the value of M_r, one of the two expressions in equation (4) is used in acoustic calculations. In the program available at Langley, these equations are written in finite difference form and are used without further modifications.

It is common practice to break down the acoustic pressure into components. Thickness, loading and skin friction noise are contributions of the terms in equation (4) involving v_n, the surface pressure p in l_i and the tangential stress due to skin friction in l_i, respectively.

Another form of the acoustic equations can be obtained by regarding the radiation field as the sum of the acoustic pressures from an array of point sources. Each point source is characterized by a volume ψ and force L_i. The points are located by slicing the blades into many small segments. Each segment has an associated volume, a force due to surface pressure and a tangential force due to skin friction. Together, these yield a point volume source and a point force source for each blade segment. The derivation of these equations from the FW–H equation was published in reference [17].

In this approach the acoustic pressure $p'(\mathbf{x}, t)$ is written as

$$p'(\mathbf{x}, t) = \sum_k (p'_{fk} + p'_{vk}), \tag{5}$$

where p'_{fk} is the acoustic pressure due to the point force of the kth segment producing loading and skin friction noise and p'_{vk} is the acoustic pressure due to the volume of that segment (producing thickness noise). These two terms are given by

$$4\pi p'_{fk} = \left\{ \frac{1}{r} \frac{1}{(1-M_r)^2} \left[\frac{\hat{r}_i}{c} \frac{\partial L_i}{\partial \tau} + \frac{L_i \hat{r}_i}{(1-M_r)} \left(\frac{\hat{r}_i}{c} \frac{\partial M_i}{\partial \tau} \right) \right] + \frac{1}{r^2} \frac{1}{(1-M_r)^2} \left[r_j L_j \frac{1-M_i^2}{1-M_r} - L_i M_i \right] \right\}_{\text{ret}}, \tag{6a}$$

$$4\pi p'_{vk} = \rho_0 \frac{\partial^2}{\partial t^2} \left[\frac{\psi_k}{r(1-M_r)} \right]_{\text{ret}} = \rho_0 \left\{ \frac{1}{1-M_r} \frac{\partial}{\partial \tau} \left[\frac{1}{1-M_r} \frac{\partial}{\partial \tau} \left(\frac{\psi_k}{r(1-M_r)} \right) \right] \right\}_{\text{ret}}, \tag{6b}$$

where ψ_k is the volume of the kth blade segment. Equation (6a) is identical to Lowson's result for a point force in motion, originally published in reference [8] and used extensively by him for helicopter rotor noise calculation. The derivation of the thickness noise formulation used in equation (6b) can be found in references [17, 25]. For numerical calculations, the source time differentiations are carried out explicitly. As in the case of Lowson's result, the acceleration of the volume source, described by the term $\partial M_r/\partial \tau$, has considerable influence on the radiated sound.

4. COMPUTATIONAL METHODS

In this section a brief review of computational methods used in the two programs will be presented. The input information for both programs is identical. The following groups of input data are required: *geometric data*: (a) blade radius and planform; blade chord, thickness ratio and twist distributions as functions of radial position; (b) airfoil section description as a function of radial position; (c) observer mode of motion, stationary or moving with the propeller; *aerodynamic data*: blade surface pressure and skin friction coefficient distributions; these can be dependent on blade azimuttial angle; *operating data*: propeller RPM and forward speed. The programs differ in details and capabilities. The MIT program is for general aviation propellers having subsonic tip speed. It can handle blades with in-plane sweep. Its chief advantage is simplicity and speed of computation. The Langley program can handle supersonic blade tip speeds and the noise of advanced propellers with out-of-plane blade sweep, such as the prop-fan designed by Hamilton Standard, can be calculated. It is more complex and takes longer to execute on a computer. Some more details of these two programs follow.

4.1. THE MIT PROGRAM

The MIT program is divided into three sections: the blade description, the blade pressure signature, and the Fourier analysis. The blade is described in the input file by a polynomial expansion of its shape and by similar expansions of the in-plane and out-of-plane loading. In addition, information is included as to the mesh size for segmenting the blade.

The mesh size is varied in both the chordwise and spanwise directions so as to allow the user some flexibility in performing the calculations. For example, a rough calculation can be made with only one point per blade for design purposes, or the mesh size can be graded coarsely on the inboard stations and finely on the outboard station so as to provide an efficient computation scheme for analyzing experimental data. Ultimately, the MIT

program replaces the blade with an array of spiraling point sources, each with a unique force vector and volume. To do this the blade mid-chord is described first and blade span is divided into strips by cuts perpendicular to radii drawn to specified stations on the centerline. These strips are further divided in the chordwise direction. The blade segments are thus constructed. The volume displacement of and force on the fluid due to each blade segment are assigned to points at the centers of these segments.

The second part of the program deals with the calculation of the blade pressure signature. The observer location at time t is specified; currently the options are for a stationary observer or for one moving with the forward velocity of the propeller. For this time t, there is an associated emission time τ for each blade segment which is calculated by an iterative scheme. Given the retarded time, the contribution of a particular segment is evaluated exactly according to equation (6). A summation over all blade segments yields the pressure signature at observer time t. Numerical integration or differentiation is not needed in this scheme. The only numerical work is involved in calculating the emission time.

The above procedure is repeated for other observer times to obtain the acoustic pressure signature. Given the pressure signature, the program then computes the Fourier analysis. The spectra are also A-weighted so as to provide useful output for designers. The flow chart for this program is presented in Figure 1.

4.2. THE LANGLEY PROGRAM

In the Langley program, the propeller blade is described by first specifying the leading edge curve in the Cartesian co-ordinate system fixed to the blade. In general this is a three-dimensional curve. The airfoil shape and the geometric angle of attack are given in planes normal to the pitch change axis as shown in Figure 2. A curvilinear co-ordinate system (Q, η_2) describes the surface of each blade. Here Q is the non-dimensional distance from the leading edge (based on local chord) in a plane normal to the pitch change axis. The radial distance of this plane from the axis of rotation is η_2. The blade is subdivided by specifying ΔQ and $\Delta\eta_2$. In general the blade panels look like parallelograms rather than rectangles. Near the leading edge of the blade smaller chordwise divisions are selected. Also smaller spanwise divisions near the blade tip are needed due to the higher helical speed.

For thickness noise, the upper and lower surface panels are both used in the summation approximating the relevant integrals in equation (4). For loading and skin friction noise, only the panel on the plane of the chord was used. This was found to be appropriate since in aerodynamic calculations often only the local lift distribution is calculated. If $\boldsymbol{\eta}(Q, \eta_2)$ is the position vector for points on the surface of a blade, then the surface area of a panel is given by

$$\Delta S = |\partial\boldsymbol{\eta}/\partial Q \times \partial\boldsymbol{\eta}/\partial\eta_2|\Delta Q\Delta\eta_2. \tag{7}$$

The local unit normal used in the calculation of the normal velocity is found from:

$$\mathbf{n} = (\partial\boldsymbol{\eta}/\partial Q \times \partial\boldsymbol{\eta}/\partial\eta_2)/|\partial\boldsymbol{\eta}/\partial Q \times \partial\boldsymbol{\eta}/\partial\eta_2|. \tag{8}$$

To calculate the emission time two schemes are used. For panels with subsonic helical speeds a scheme which adjusts the source time τ to make $g = \tau - t + r/c$ approach zero is used (Newton's method). This scheme is very fast. For panels with transonic or supersonic helical speed, the method of modified regula falsi [26] is used to solve for the emission times. It was found unnecessary to calculate the emission times for upper and lower surface panels separately. The emission times of the center points of the panels on the camber surface were used for panels which lie on the actual blade surface directly above and below

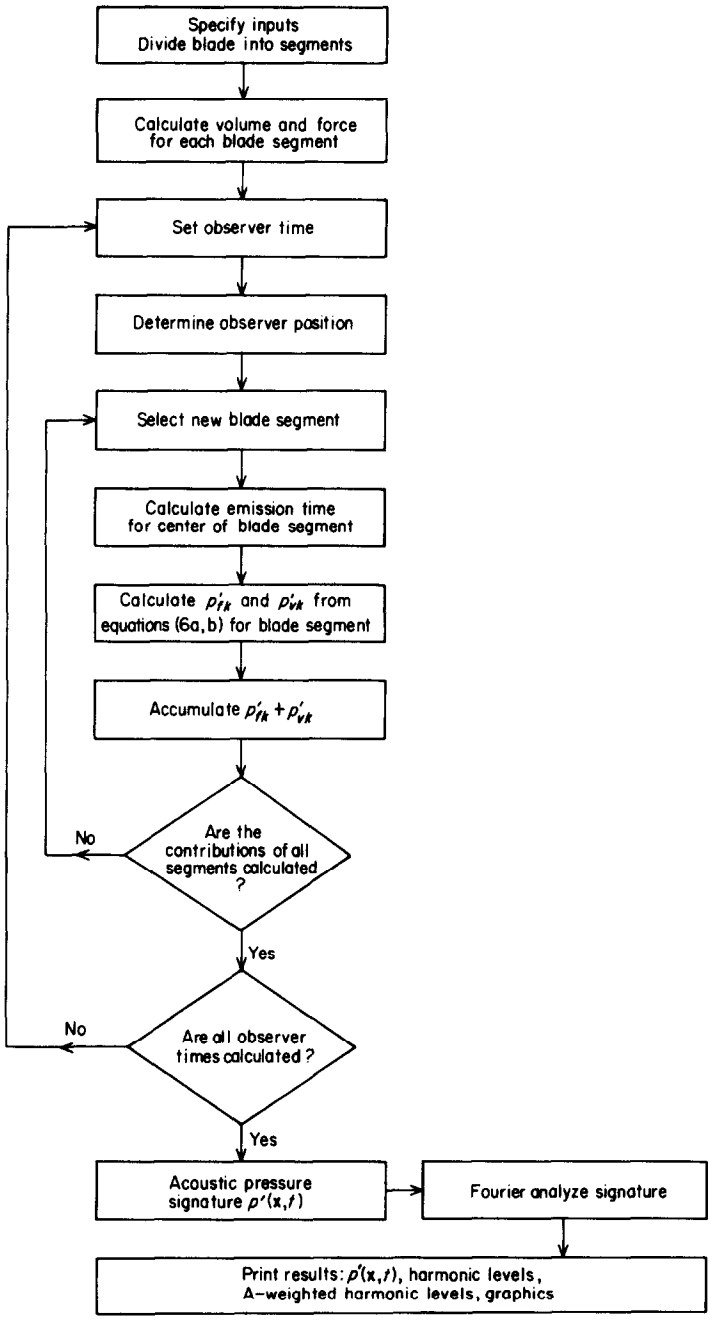

Figure 1. Flow chart for MIT acoustic program.

these panels. The two methods of finding emission times will be called schemes 1 and 2, respectively, in the flow chart for this program.

For panels with $M_r < 1$, equation (4a) is used in discrete form. Equation (4b) in discrete form is used for panels with $M_r \simeq 1$ or $M_r > 1$. In this case, the collapsing sphere method is used for each panel individually. To obtain good accuracy, at least ten intersections of the collapsing sphere and the panel are used for approximating the integrals in equation (4b). Figure 3 shows the flow chart for the Langley program.

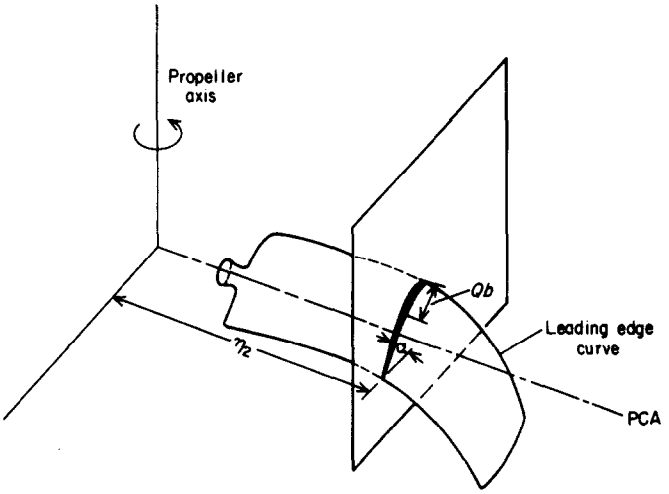

Figure 2. Curvilinear co-ordinate system (Q, η_2) used in the Langley program to describe blade geometry of advanced propellers. The blade mean surface is not in a plane. α, Geometric angle of attack (function of η_2); PCA, pitch change axis; b, chord (function of η_2); Q, distance from L.E./b.

The Langley program is more complex and is slower than the MIT program. Comparison of the outputs of MIT and Langley programs with identical inputs have convinced the authors that the results of the two programs are virtually identical for propellers with subsonic helical tip speeds.

Both the Langley and the MIT programs can handle cases where the observer is in motion with the propeller. This is achieved by noting that if $\mathbf{x}_m$ is the position of the observer in the moving frame, then the observer position in the frame fixed to the undisturbed medium is

$$\mathbf{x}_f = \mathbf{x}_m + \int_0^t \mathbf{v}(t')\,\mathrm{d}t', \tag{9}$$

where $\mathbf{v}(t')$ is the forward velocity of the propeller. Therefore in the moving frame $p'(\mathbf{x}_m, t) = p'(\mathbf{x}_f, t)$. Note that $\mathbf{x}_f = \mathbf{x}_f(\mathbf{x}_m, t)$ and this is known if the motion of the propeller is specified.

5. COMPARISON WITH EXPERIMENTAL DATA

In this section theoretical calculations of propeller noise will be compared with measured acoustic data for a conventional propeller and an advanced propeller.

5.1. A GENERAL AVIATION PROPELLER

This set of measurements is well documented [21]. A twin-engine, high wing, light STOL transport was used with two microphones on the portside wing tip, one in the propeller plane at 7·28 m from the axis of rotation. The second microphone was at the same distance from the propeller axis but 3·05 m behind the propeller plane. The flight tests were conducted with the starboard engine shut down. The propeller had three blades with a diameter of 2·59 m and its RPM (100%) was 2200. The blade form curves are shown in Figure 4. One blade was instrumented with seven pressure transducers which responded to local surface pressure variation on the pressure side of the blade.

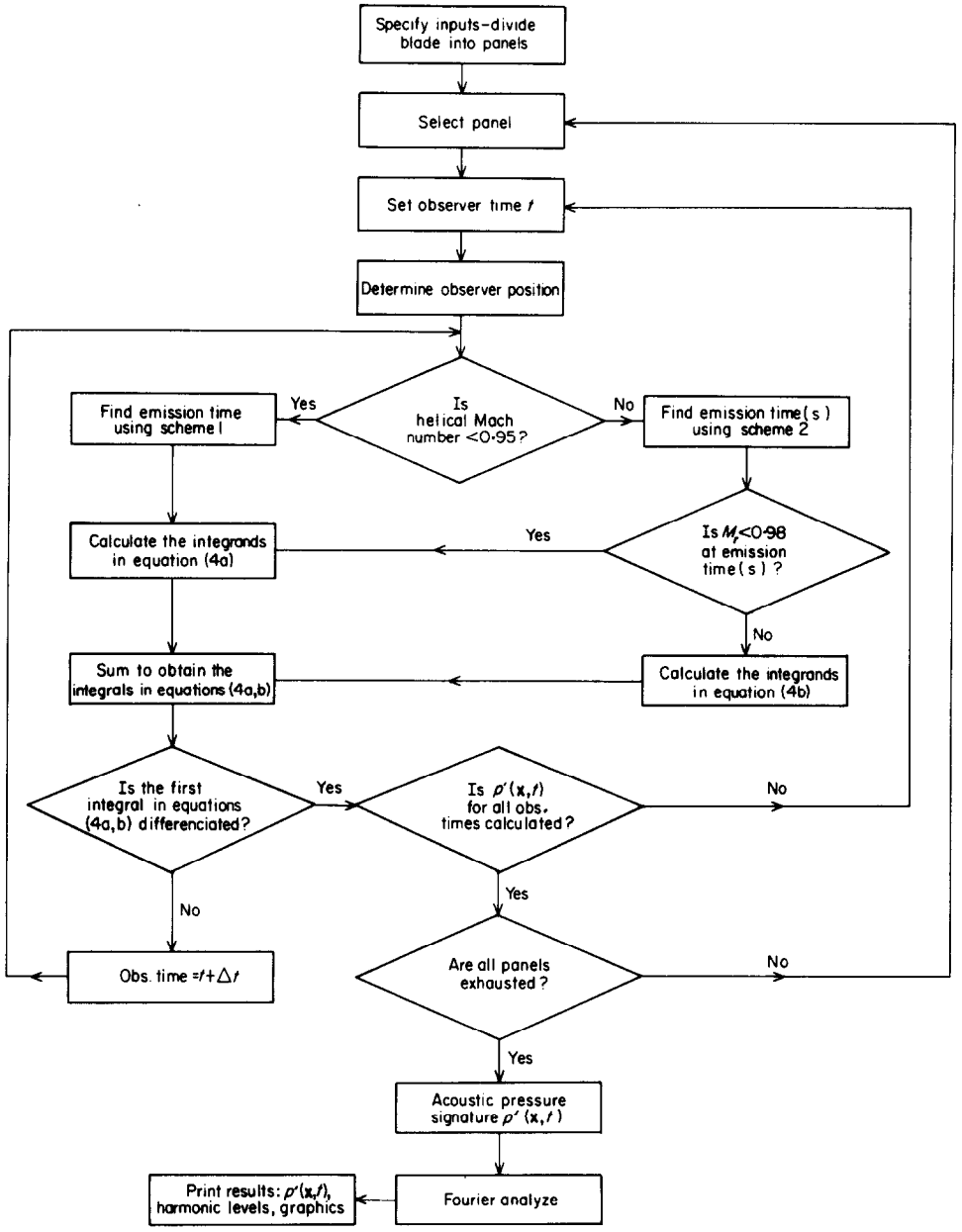

Figure 3. Flow chart for Langley acoustic program.

For comparison, five tests were selected from the published test report [21]. To reduce confusion, the same run number designations are used in this paper as in that report. Table 1 summarizes the operating conditions for the test runs. The acoustic pressure spectra for the two microphones for all test runs are available in reference [21]. Some acoustic pressure signatures were produced from recorded test data for this paper. The MIT program was used to obtain the theoretical acoustic pressure signatures and spectra.

The aerodynamic calculations are based on a vortex theory described by Larrabee [27]. The net thrust and torque in Table 1 are calculated by this method for which the propeller is assumed to be operating at minimum induced loss. To the authors' knowledge, there are

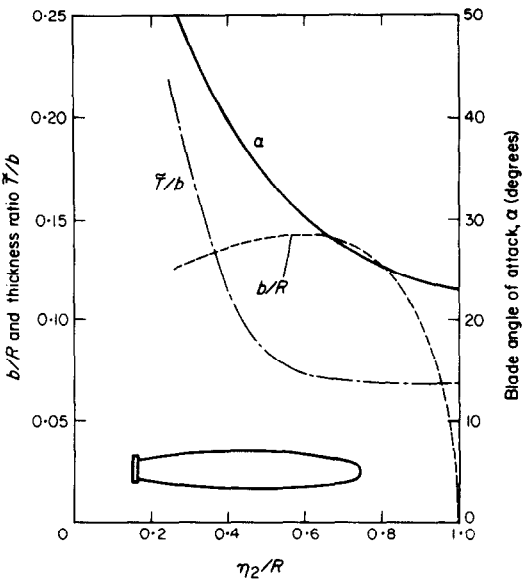

Figure 4. Blade form curves and the planform for the general aviation propeller used for in-flight acoustic measurement. b, Chord; $\bar{T}$, maximum thickness of airfoil; R, blade radius; η_2, distance from propeller center.

no reliable in-flight aerodynamic data for propellers to substantiate this assumption. However, the calculated radial distributions of the blade loads for five runs, shown in Figure 5, appear reasonable. This approximation was made only to expedite the calculation. A more accurate estimate of the propeller loading is necessary for greater accuracy in noise prediction. The radial load developed by propellers operating at

TABLE 1

Operating conditions for in-flight test of the general aviation propeller (the aircraft was flown on one engine); full rpm (100%) = 2200

Run	Ambient pressure ($Pa \times 10^{-5}$)	Ambient temperature (deg K)	Relative humidity (%)	Wind speed (kt)	% rpm	Power (kW)
2	1·021	305	56	4	97·5	363
3A	1·0232	296	47	10	80·0	249
8	1·0231	296	47	10	97·5	392
9	1·0231	296	47	10	80·0	262
10	1·0231	296	47	10	97·5	262

Run	Forward speed (kt)	Aircraft altitude (m)	Calculated torque per blade (Nm)	Calculated thrust per blade (N)	Helical tip Mach number
2	121	61	538·7	1610·4	0·85
3A	97	61	450·3	1344·2	0·71
8	124	305	581·7	1703·4	0·86
9	97	305	473·8	1403·9	0·71
10	97	305	388·8	1385·1	0·86

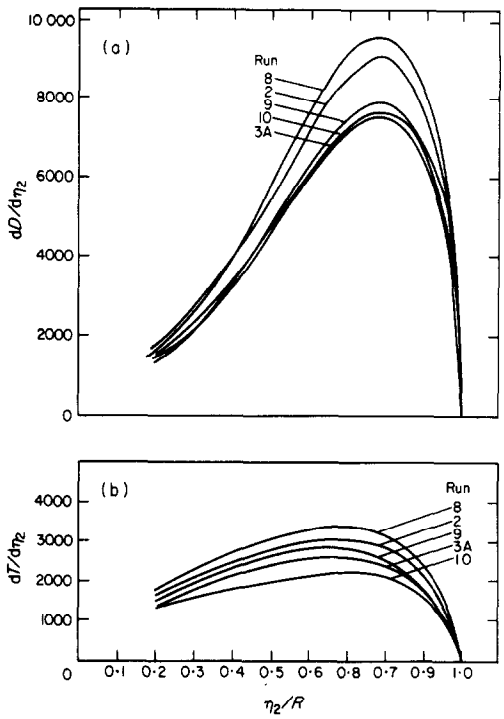

Figure 5. Calculated variation of blade loads as a function of normalized distance from propeller center η_2/R for the five tests of the general aviation propeller. (a) Axial forces; (b) disk plane forces. D, Drag; T, thrust; R, blade radius.

arbitrary conditions can be calculated. One prediction scheme is that given in Larrabee's paper [27].

In the aerodynamic theory of propellers one assumes that the lift vector is not perpendicular to the kinematic velocity of the blade section. The perturbation to the flow field by the propeller must be included in calculating the velocity field; hence the lift is perpendicular to the total velocity which is the vector sum of the kinematic velocity plus the induced velocity. Given the lift vector, the surface friction effects are included in the standard manner by assuming they are perpendicular to the lift vector and equal in magnitude to (C_D/C_L) times the lift force. The drag-to-lift ratio used in the calculations was the optimum (C_D/C_L) for the series 16 airfoil used on this propeller.

An approximation was made in that the chordwise distribution of the friction forces was assumed to be identical to the lift forces. This approximation is not critical as the calculation of the pressure signature is much more sensitive to the radial load distribution. The chordwise blade description is much more important in calculating the thickness noise. This noise is sensitive to chordwise variations of the volume distribution at tip speeds greater than Mach 0·75. The contribution of the friction forces to the overall noise of the propeller was so small that it could be neglected in acoustic calculations. This is in agreement with the findings of Farassat *et al.* [28]. However, in the results reported here it was added to the loading noise and not calculated separately.

The test result showed that due to flow assymmetry, the unsteady part of the surface pressure varied in phase for all transducer positions almost sinusoidally. The flow asymmetry was caused by engine blockage and the frequency of the variation was the same as the shaft frequency. The positive peak appeared when the blade was in the third quadrant of the propeller disk when viewed from the front. The amplitude of this pressure

variation was large enough to produce a large variation in blade load. It was estimated that the amplitude of the first harmonic blade load varied up to 20% of the steady load. Higher harmonics of the load variation were negligible. For this reason, in the following calculations, this unsteady loading component is included. Note that in all the theoretical results, the observer is in motion with the propeller.

A study of the effect of mesh size variation on the acoustic pressure signature was done to select proper chordwise mesh sizes for calculations reported here. For this study, 13 radial stations were used. The number of chordwise divisions varied from the hub to the tip. These divisions were selected so that the chordwise separations between consecutive points on the effective planform were approximately equal. The effective (acoustic) planform has a maximum chordwise length when the blade is approaching the observer at maximum speed. This effective chord is roughly equal to the actual chord divided by $[1-(\eta_2/R)M_{tip}]$, where η_2 is the radial distance and M_{tip} is the propeller tip Mach number. The chordwise divisions were increased until no noticeable change appeared in the calculated acoustic pressure signature. In the case of the results reported in this section, as little as 5 chordwise divisions at the blade tip and 1 division near the hub was found to be sufficient. The study has shown that chordwise mesh size does have influence on the results of the acoustic calculations. First, the coarser the mesh size, the sharper the loading and thickness noise signatures. Here the signal sharpness is defined for loading noise as peak-to-peak difference divided by the interval between peaks. For thickness noise, the sharpness is defined as the magnitude of the negative pulse divided by signal width at half the peak value. If, as is often the case, there is asymmetry in chordwise loading and thickness distributions with respect to the midchord point, then the effect of varying mesh sizes is to change the zero crossing time of the acoustic pressure signature. Finally, although the individual components of the noise appear to change by mesh size variation, the effect on overall pressure signature may be less significant due to cancellation of signals of opposite sign.

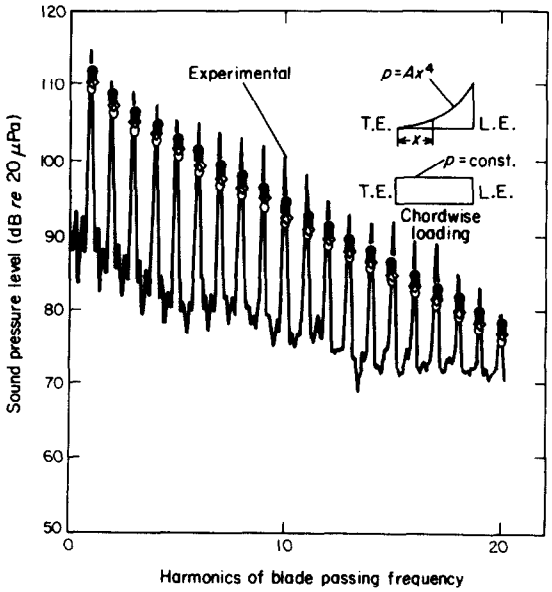

Figure 6. The effect of chordwise loading and unsteady blade load variation on the calculated acoustic pressure spectrum and comparison with measured spectrum for run 8. In-plane microphone. ●, Peak unsteady; ■, peak, steady; ◇, uniform, unsteady; ○, uniform, steady.

Figure 6 shows the influence of the chordwise loading and the unsteady loading discussed above on the calculated noise for run 8. It is seen that for uniform loading, the inclusion of unsteady loading has increased the level of all the calculated harmonics only very slightly. For a more realistic chordwise distribution which peaks at the blade leading edge (of the form Ax^4, where A is a constant and x is the distance from the T.E.), there is further increase in the level of high harmonics of the calculated noise. This fact was pointed out by Hanson [18] but has been known for some time [29, p. 194].

The unsteady loading influences both low and high order harmonics. It is important to realize that the addition of a periodic unsteady load breaks the azimuthal symmetry of the sound field. Suppose the observer is in the disk plane at a given radius from the axis of symmetry. The level detected depends on the difference between the azimuthal location of the unsteady load and the observer azimuth. The unsteady loading influences the sound level in two ways. First, there is a term proportional to $\partial L_i/\partial\tau$ (see equation (6a)) whose greatest effect is to radiate sound in the direction normal to the propeller disk. Next the unsteady load affects the magnitude of the force L_i at any given time. In the case of Figure 6 (run 8) the load is adjusted so that the maximum L_i occurs when the blade is approaching the wing tip microphone at its fastest rate. This leads to a net increase in calculated sound level at both low and high harmonics.

Figures 7 and 8 show the calculated and measured acoustic pressure signatures and spectra for runs 2 and 3A. The agreement of the calculated and measured results is very good. The signatures for loading and thickness noise of run 2 are presented in Figure 9. One can see that both thickness and loading noise are of the same order of magnitude and

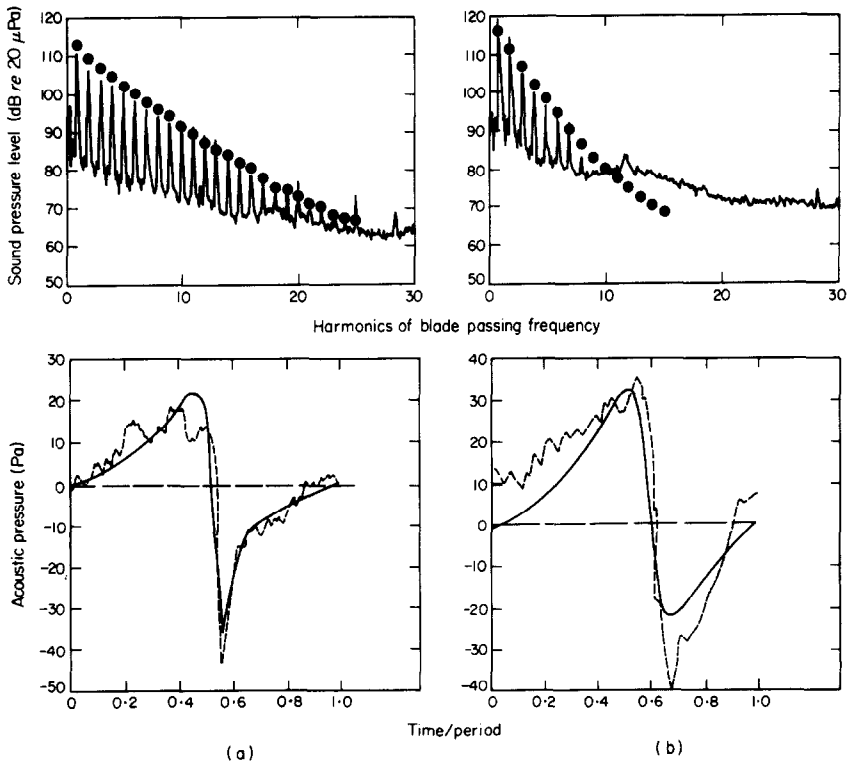

Figure 7. Calculated and measured acoustic spectra (top) and pressure signatures (bottom) for the general aviation propeller, run 2. (a) In-plane microphone, period = 9·32 ms; (b) aft microphone. For spectra: ——, experimental; ●, theoretical; for pressure signatures: – – –, experimental; ——, theoretical.

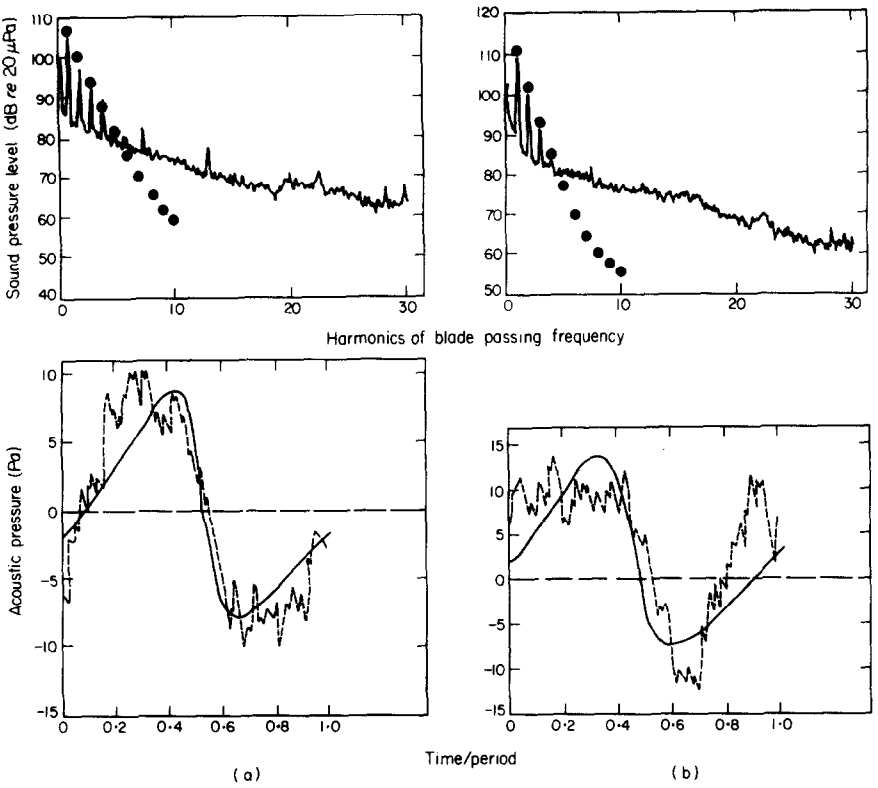

Figure 8. Calculated and measured acoustic spectra (top) and pressure signatures (bottom) for the general aviation propeller, run 3A. (a) In-plane microphone, period = 11·36 ms; (b) aft microphone. Legend as for Figure 7.

neither can be neglected in calculations. In all theoretical calculations, a chordwise loading with the peak at the leading edge has been used.

It is well-known that the blade tip speed strongly influences the noise of propellers. This can be seen in Figure 10 where the two acoustic pressure spectra presented correspond to

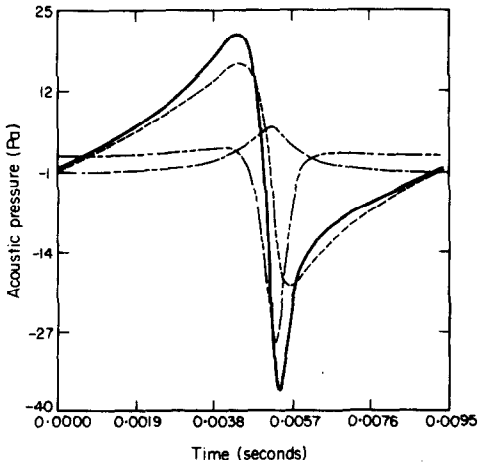

Figure 9. Relative magnitudes of loading and thickness noise for in-plane microphone position, run 2. The effect of skin friction is included in the loading noise. — — —, Far field loading noise; — — —, near field loading noise; — — — —, thickness noise; ——, total noise.

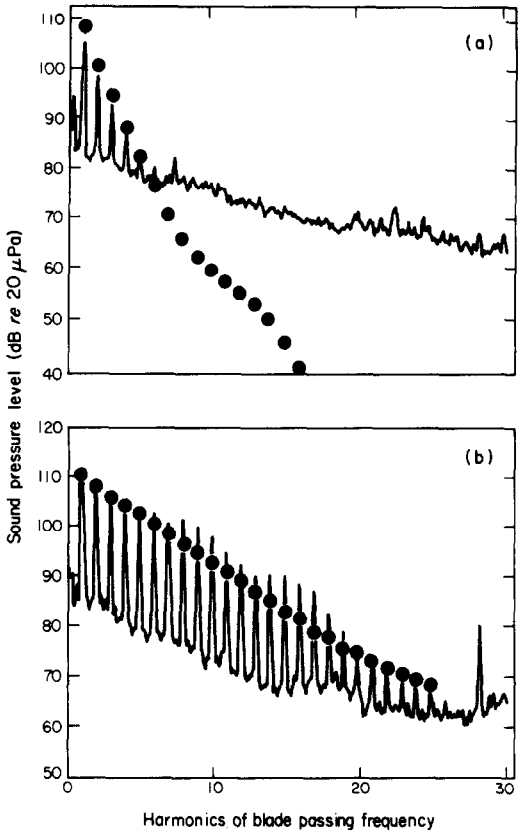

Figure 10. Comparison of theoretical and measured acoustic spectra for two different helical tip speeds, in-plane microphone. (a) Run 9, $M_t = 0{\cdot}71$; (b) run 10, $M_t = 0{\cdot}86$. —, Experimental; ●, theoretical.

helical tip speeds of (a) 190·9 m/s and (b) 230·1 m/s. In the latter case, the acoustic spectrum falls off less rapidly and the overall noise level is considerably higher than that of the lower tip speed case.

On the whole, it can be said that the in-flight propeller noise of general aviation aircraft can be predicted with reliable precision. One should have some knowledge of aerodynamic blade load variation due to either the influence of flow around the aircraft or the propeller plane oblique angle with free stream velocity vector. Apart from loading noise, thickness noise must be included in calculations but the skin friction noise is negligible.

5.2. AN ADVANCED PROPELLER

The Langley program was used to calculate the noise of a prop-fan designed by Hamilton Standard. Acoustic test data for a 2-bladed model prop-fan (SR-1 Model) with swept blade were supplied by the manufacturer. The data were collected in the United Technologies Research Center open jet anechoic tunnel. The jet Mach number was 0·32 (106·3 m/s). The blade radius was 0·31 m and the helical tip speed of the model was 343·7 m/s ($M = 1{\cdot}03$). The blade form curves and a sketch of the untwisted planform are presented in Figure 11. This design was not acoustically optimized and was used to study the effectiveness of blade sweep in reducing the radiated noise. The calculated radial distribution of blade lift coefficient is presented in Figure 12. The net torque, thrust and power of the model were 37 Nm, 325 N and 39 kW respectively. The microphones were outside the tunnel jet shear layer.

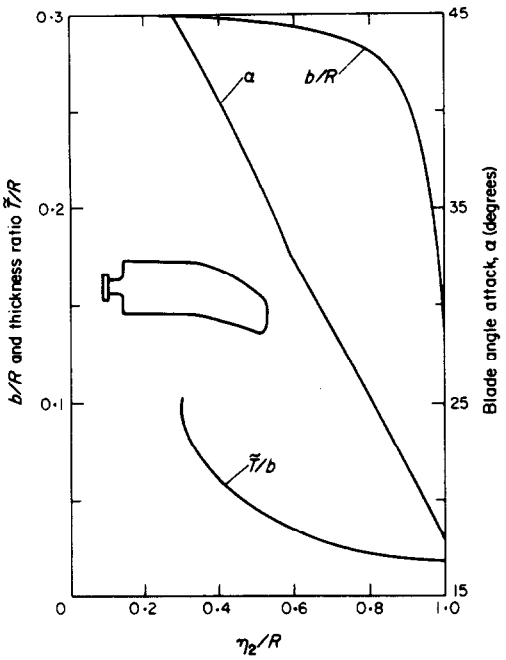

Figure 11. Blade form curves and the planform for the advanced propeller. b, Chord; $\tilde{T}$, maximum thickness of airfoil; R, blade radius; η_2, distance from propeller center.

Figures 13(a) and (b) present the calculated and measured acoustic pressure signatures and spectra for two microphone positions. The microphone positions and the level of the measured noise harmonics have been corrected for the tunnel jet shear layer effect by using Amiet's theory. The microphone positions shown in the figures, which were used in the theoretical calculations, correspond to positions where the microphones would be if the jet diameter were large enough to enclose them. These corrections were supplied by the manufacturers also. The moving microphone option of the acoustic program was therefore used for these calculations. The chordwise loading was assumed to be parabolic. This assumption was probably not realistic. There are little theoretical or experimental

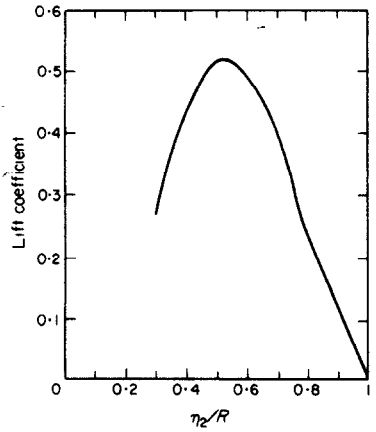

Figure 12. Radial distribution of blade lift coefficient for the advanced propeller. η_2, Distance from propeller center.

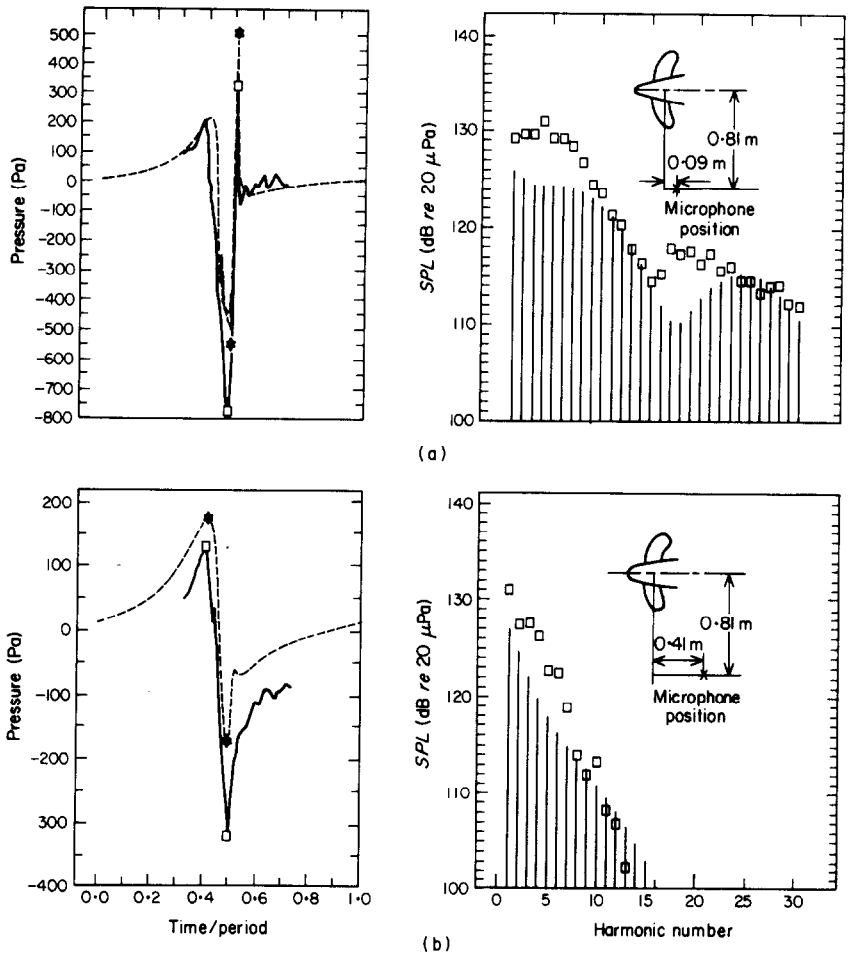

Figure 13. Comparison of theoretical and experimental acoustic pressure signatures and spectra for the advanced propeller. Period, 2·667 ms; number of blades, 2. For signatures: —□—, experimental; - - - ★ - - -, theoretical; for spectra: □, experimental; |, theoretical. (a) Microphone position 0·09 m from propeller plane; experimental *OASPL* = 139·1; theoretical, *OASPL* = 135·5; (b) microphone position 0·41 m from propeller plane; experimental *OASPL* = 135·2; theoretical *OASPL* = 130·9. All *OASPL*'s dB *re* 20 μPa.

aerodynamic data on thin airfoils in the range of Mach numbers encountered in the test. Therefore, this assumption must be considered one source of error. These two figures present typical results of many similar calculations.

From these figures, it is seen that the theoretical pressure signatures closely resemble the measured signatures. The theoretical and measured acoustic spectra also show reasonably good agreement, with some exceptions. The level of the low harmonics of the acoustic spectrum is underestimated by about 5 dB in Figure 13(a). This discrepancy is more pronounced where thickness noise is the dominant component of the noise. It is now generally believed that this is a non-linear flow effect. Yu *et al.* [23] and Hanson and Fink [24] have attempted to account for this discrepancy by including in their acoustic calculations the quadrupole source term appearing in the FW–H equation. This approach requires almost as much effort as needed to solve the flow problem around the blades, which would make the acoustic calculations redundant.

Another point of disagreement between the measured and calculated acoustic spectra is that the first dip in the experiment spectrum appears at a lower frequency than that of the

calculated spectrum. This is related to the width of the main pulse in the acoustic pressure signature which is larger in the measured than in the calculated signature. This disagreement is also believed to be due to flow non-linearities which are neglected in acoustic calculations. This weakness of linear acoustic theory to account properly for the width of the main pulse of the pressure signature was pointed out by Boxwell, Yu and Schmitz [30].

Although linear acoustic theory has some shortcomings, it can be a very useful tool in the design stage of propellers. It is believed that the noise regulations for propeller-driven aircraft will be based on flight conditions. The methods presented here will be suitable for estimation of the noise of these aircraft.

6. CONCLUDING REMARKS

In this paper two methods have been described for the calculation of propeller noise. The formulations used in these methods and a brief discussion of the algorithms employed in two computer programs developed at MIT and at Langley have been presented. The programs differ in capability and complexity. The main difference between the two programs is that the MIT program can only handle propellers with subsonic tip speed but the Langley program can also treat propellers with supersonic tip speed. All the acoustic calculations are performed in the time domain. In subsonic cases, no noticeable differences between the outputs of the two programs have been observed.

The noise of conventional propellers in forward flight can be predicted with good accuracy by taking account of only thickness and loading noise sources. A non-compact source formulation which accounts for differences in emission time for sources on the blade surface must be used. Low harmonics of blade loading due to flow asymmetry into the propeller must be included. The examples in this paper have shown that the thickness noise is an important component of the overall noise of conventional propellers. The noise due to tangential skin friction stress is negligible. It must be remembered that in general aviation aircraft there are sources of sound other than propellers, such as the engine, which may influence the measured noise spectra considerably. These sources have not been discussed here.

For propellers with high tip speeds, linear acoustic theory, which is used in the two programs discussed here, does provide good estimates of the radiated noise. There are two features of the measured acoustic pressure signature and spectrum that the linear theory does not account for. First, the calculated width of the main pulse of the pressure signature is narrower, and second the levels of the first few harmonics of the acoustic pressure spectrum are in many cases underestimated. Both these two features, which are believed to be due to non-linearities in the flow around the blades, are prominent where the thickness noise component is significant. The deviations between measured and calculated results appear at transonic and supersonic tip speeds. Nevertheless, many acoustic calculations for propellers with advanced and conventional blade design have convinced the authors that the methods presented here, when the results are properly interpreted with good engineering judgment, provide useful tools in estimating propeller noise in flight.

ACKNOWLEDGMENTS

The works of G. P. Succi and F. Farassat were supported by NASA Contract No. NASI-15154 and NASA Research Grant NSG 1474, respectively. F. Farassat would like to thank Mr P. A. Nystrom of the Acoustics and Noise Reduction Division of NASA Langley Research Center for his technical support. The help of the staff of the acoustics

group of Hamilton Standard, particularly Mr F. B. Metzger and Dr D. B. Hanson for supplying technical data on the prop-fan, is gratefully acknowledged.

REFERENCES

1. C. L. MORFEY 1973 *Journal of Sound and Vibration* **28**, 587–617. Rotating blades and aerodynamic sound.
2. L. GUTIN 1936 *Zhurnal Technicheskoi Fiziki* **6**, 899–909. (in Russian) (Translated as 1948 *NACA TM* 1195. On the sound field of a rotating airscrew.)
3. W. ERNSTHAUSEN 1936 *Luftfahrtforschung* **8**, 433–440. (in German) (Translated as 1937 *NACA TM* 825. The source of propeller noise.)
4. A. F. DEMING 1938 *NACA TM* 679. Noise from propellers with symmetrical sections at zero blade angle, II.
5. I. E. GARRICK and C. E. WATKINS 1954 *NACA Report* 1198. A theoretical study of the effect of forward speed on the free-space sound-pressure field around propellers.
6. R. A. ARNOLDI 1956 *United Aircraft Corporation Research Department, East Hartford, Connecticut, Report R*-0896-1. Propeller noise caused by blade thickness.
7. A. I. VAN DE VOOREN and P. J. ZANDBERGEN 1963 *American Institute of Aeronautics and Astronautics Journal* **1**, 1518–1526. Noise field of a rotating propeller in forward flight.
8. M. V. LOWSON 1965 *Proceedings of the Royal Society (London)* **A286**, 559–572. The sound field for singularities in motion.
9. J. E. FFOWCS WILLIAMS and D. L. HAWKINGS 1969 *Philosophical Transactions of the Royal Society (London)* **A264**, 321–342. Sound generated by turbulence and surfaces in arbitrary motion.
10. W. F. MÖHRING, E. A. MÜLLER and F. F. OBERMEIER 1969 *Acustica* **21**, 184–188. Schallerzeugung durch instationare Stromung als singulare storungs Problem.
11. R. H. LYON 1971 *Journal of the Acoustical Society of America* **49**, 849–905. Radiation of sound by airfoils that accelerate near the speed of sound.
12. D. L. HAWKINGS and M. V. LOWSON 1974 *Journal of Sound and Vibration* **36**, 1–20. Theory of open supersonic rotor noise.
13. F. FARASSAT 1975 *NASA Technical Report R*-451. Theory of noise generation from moving bodies with an application to helicopter rotors.
14. D. B. HANSON 1976 *American Institute of Aeronautics and Astronautics Paper* 76-565. Near field noise of tip speed propellers in forward flight.
15. Y. NAKAMURA and A. AZUMA 1978 *NASA Conference Publication* 2052, 323–337. Improved method for calculating the thickness noise.
16. C. J. WOAN and G. M. GREGOREK 1978 *American Institute of Aeronautics and Astronautics Paper* 78-1122. The exact numerical calculation of propeller noise.
17. G. P. SUCCI 1979 *Society of Automotive Engineers Paper* 790584. Design of quiet efficient propellers.
18. D. B. HANSON 1979 *American Institute of Aeronautics and Astronautics Paper* 79-0609. The influence of propeller design parameters on far field harmonic noise in forward flight.
19. W-H. JOU 1979 *American Institute of Aeronautics and Astronautics Paper* 79-0348. Supersonic propeller noise in a uniform flow.
20. D. B. HANSON 1975 *American Institute of Aeronautics and Astronautics Paper* 75-468. Study of subsonic fan noise sources.
21. D. MAGLIOZZI 1977 *NASA Contractor Report* 145105. The influence of forward flight on propeller noise.
22. R. J. PEGG, B. MAGLIOZZI and F. FARASSAT 1977 *American Institute of Mechanical Engineers Paper* 77-*GT*-70. Some measured and calculated effects of forward velocity on propeller noise.
23. Y. H. YU, F. X. CARADONNA and F. H. SCHMITZ 1978 *Fourth European Rotor Craft and Powered Lift Aircraft Forum, Stressa, Italy, Paper No.* 58. The influence of the transonic flow field on high-speed helicopter impulsive noise.
24. D. B. HANSON and M. R. FINK 1978 *Presented at the Spring Meeting of the Institute of Acoustics, Cambridge University, England.* The importance of quadrupole sources in prediction of transonic tip speed propeller noise. (Also 1979 *Journal of Sound and Vibration* **62**, 19–38.)
25. F. FARASSAT 1977 *Journal of Sound and Vibration* **55**, 165–193. Discontinuities in aerodynamics and aeroacoustics: the concept and applications of generalized derivatives.

26. S. D. CONTE and C. DE BOOR 1972 *Elementary Numerical Analysis.* New York: McGraw-Hill Book Company, second edition.
27. E. LARRABEE 1979 *Society of Automotive Engineers Paper* 790585. Practical design of minimum induced loss propellers.
28. F. FARASSAT, C. E. K. MORRIS and P. A. NYSTROM 1979 *American Institute of Aeronautics and Astronautics Paper* 79-0608. A comparison of linear acoustic theory with experimental noise data for a small scale hovering rotor.
29. E. J. RICHARDS and D. J. MEAD (editors) 1968 *Noise and Acoustic Fatigue in Aeronautics.* London: John Wiley and Sons Limited.
30. D. A. BOXWELL, Y. H. YU and F. H. SCHMITZ 1978 *NASA CP* 2052, 309–322. Hovering impulsive noise—some measured and calculated results.